

Position-Based Routing on 3-D Geometric Graphs in Mobile Ad Hoc Networks

George Kao*

Thomas Fevens*

Jaroslav Opatrny*

Abstract

A unit disk graph and its proximity graphs are often used as the underlying topologies of a mobile ad hoc network. One category of unicast routing algorithms, position-based routing algorithms, has been developed and studied extensively in the context of 2-D. This, however, poses evident questions in terms of the reliability and efficiency of these algorithms when practically the mobile host is an object positioned in the real world of 3-D. We propose a heuristic for routing in 3-D based on the 2-D face routing algorithm. We study experimentally the properties of geometric graphs in 3-D and the performance of various routing algorithms on these graphs.

KEYWORDS: three-dimension; geometric spanning subgraph; routing algorithm; mobile ad hoc network.

1 Introduction

A wireless mobile ad hoc network (MANET) consists of mobile hosts that communicate with each other without fixed infrastructure or centralized control. A mobile host usually operates as a router and is able to communicate with another mobile host if the distance between them is within the minimum of their two direct transmission ranges. As the mobile hosts move frequently, the underlying topology of the network may change. Routing efficiently in such network becomes a challenging task.

Several geometric graphs that represent the underlying topologies [2] of a MANET and many routing algorithms have been proposed and studied in 2-D during the past few years. Our goal is to extend these geometric graphs and routing algorithms to 3-D as they can better represent the real-world scenarios.

Assuming that all mobile hosts have the same maximum transmission range R , a MANET can be modeled as a unit disk graph (UDG). Let n be the number of mobile hosts. The number of edges in the UDG could be as large as $O(n^2)$, i.e., a fully connected topology, if the maximum distance between any pair of mobile hosts is less than R .

In the routing algorithms that adopt the flooding strategy, a mobile host forwards a packet to all its neighbors in the network to discover a path, which potentially incurs high communication overhead. One method to reduce such overhead is to allow each mobile host to communicate only with a selected subset of the neighboring mobile hosts. This approach can be seen as retaining geometric spanning subgraphs, such as Gabriel graph (GG) [5] and relative neighborhood graph (RNG) [7], of the UDG. Both GG and RNG, extracted from the UDG, can be computed in a distributed manner.

In this paper, a heuristic for face routing in 3-D is proposed. This projective face routing algorithm, by our simulation, gives significantly better delivery rate than the other routing algorithms. The rest of paper is organized as follows. Section 2 defines geometric graphs in 3-D. In section 3, we review the localized position-based routing algorithms and describe our proposed heuristic. We present our experimental results in section 4 and finally conclude the paper in section 5.

2 Geometric Graphs in 3-D

A MANET is represented by a geometric undirected graph [1], $G = (V, E)$. Each mobile host with x -, y - and z -coordinates is a point (x, y, z) in the Euclidean space. If there is a bidirectional communication link between any pair of mobile hosts, an edge connects the pair of points that represent the hosts. We define $d(u, v)$ as the Euclidean distance between the points u and v ,

$$d(u, v) = \sqrt{(u_x - v_x)^2 + (u_y - v_y)^2 + (u_z - v_z)^2}. \quad (1)$$

We also define $S(p, r)$ as the sphere with center point p and radius r .

The spanning subgraphs, GG and RNG, extracted from UDG can be calculated locally by using only the location information of 1-hop neighbors. If $\{u, v\}$ is an edge in UDG, only the 1-hop neighbors of the point u or v are required to test if the edge $\{u, v\}$ is to be removed. As long as UDG is a connected graph, the connectivity of GG and RNG is also preserved.

Unit Disk Graph (UDG) Assume that the maximum transmission range for each mobile host is R . Any other point that is inside the sphere $S(u, R)$

*Department of Computer Science, Concordia University, 1455 De Maisonneuve Blvd. West, Montreal, Quebec, Canada, H3G 1M8. [geor_kao, fevens, opatrny]@cs.concordia.ca

connects to the point u . The set of edges E , representing the communication links, of the UDG satisfies $\{\{u, v\} : u, v \in V, d(u, v) \leq R\}$.

Gabriel Graph (GG) Let q be the mid-point of an edge $\{u, v\}$. The edge $\{u, v\}$ exists between the points u and v if no other point w is present inside the sphere $S(q, \frac{d(u, v)}{2})$. The set of edges E of GG satisfies $\{\{u, v\} : u, v \in V, d(u, v) \leq \min_{w \in V - \{u, v\}} \{\sqrt{d^2(u, w) + d^2(v, w)}\}\}$.

Relative Neighborhood Graph (RNG) An edge $\{u, v\}$ exists between the points u and v if no other point w is present inside the lune formed by the intersection of the two spheres, $S_u(u, d(u, v))$ and $S_v(v, d(u, v))$. The set of edges E of RNG satisfies $\{\{u, v\} : u, v \in V, d(u, v) \leq \max_{w \in V - \{u, v\}} \{d(u, w), d(v, w)\}\}$.

3 Localized Position-Based Routing Algorithms

Localized position-based routing algorithms [6] are distributed algorithms. Each host makes the routing decision solely based on the location information of itself, its neighbors, the source and the destination. Let u be the current node, (v_1, \dots, v_n) be the 1-hop neighboring nodes of u , s be the source node and t be the destination node. The hop counts of the path discovered by the algorithm between the nodes s and t is denoted by $N_L(s, t)$. The hop counts of the shortest path between the nodes s and t is denoted by $N_D(s, t)$. We define the hop stretch factor as $SF(s, t) = \frac{N_L(s, t)}{N_D(s, t)}$. We now specify four well-known routing algorithms that are used for a comparison with the routing algorithm proposed in this paper.

3.1 Compass Routing [9]

The current node u selects its neighboring node that forms the smallest angle, $\min\{\angle v_1ut, \dots, \angle v_nut\}$, together with the destination node t .

3.2 Greedy Routing [4]

The current node u selects its neighboring node that is the closest, $\min\{d(v_1, t), \dots, d(v_n, t)\}$, to the destination node t .

3.3 Ellipsoid Routing [11]

The current node u selects its neighboring node that gives the smallest sum of distances, $\min\{d(v_1, u) + d(v_1, t), \dots, d(v_n, u) + d(v_n, t)\}$, from itself to the neighboring node and then to the destination node t .

3.4 Most Forward Routing [10]

Let (v'_1, \dots, v'_n) be the nodes projected on the line ut respectively. The current node u selects its neighboring node whose projected node is the closest, $\min\{d(v'_1, t), \dots, d(v'_n, t)\}$, to the destination node t .

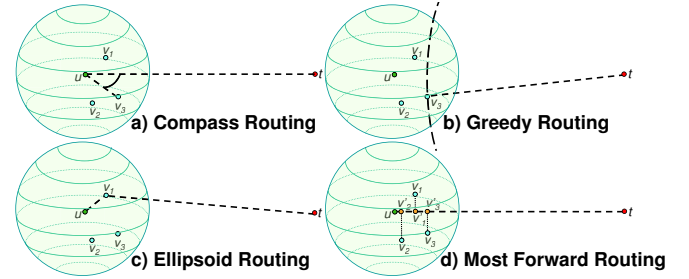


Figure 1: Various routing algorithms.

3.5 Projective Face Routing

Face routing [3, 8], by using the right-hand rule, guarantees the delivery on a 2-D geometric planar graph. The line st that connects the source and destination nodes determines the 2-D faces to be traversed. However, this line does not determine these faces in a 3-D graph. This algorithm is thus not directly applicable on a 3-D graph.

We propose a heuristic using the projective approach to deal with the problem described above. Although this approach does not guarantee the delivery as a planar graph cannot be extracted from the projected graph using only its local information before projection (see Figure 2), our experiments show that the delivery rate is significantly better than the other routing algorithms. By delivery rate, we mean the percentage of successful deliveries to the destination. The algorithm is as follows. The points are first projected onto one plane that contains the line st . The face routing is performed on this projected graph. If the routing fails, the points are then projected onto the second plane, that is orthogonal to the first plane and also contains the line st . The face routing is again performed.

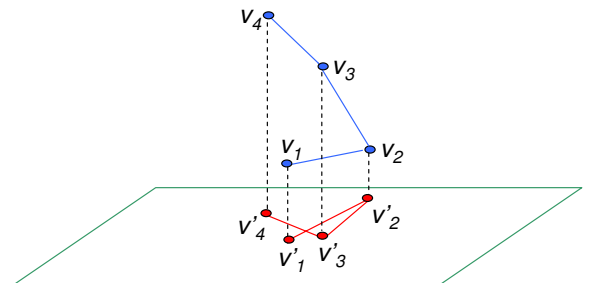


Figure 2: Projective face routing algorithm. The neighboring nodes are preserved after projection.

4 Experimental Results

4.1 Simulation Environment

We conduct experiments under uniform distribution. There are 75 nodes randomly generated in a cube of side length 100. The maximum transmission radius of each host is set to a fixed value. We first calculate all connected components in the graph so that we can identify the number of maximal connected subgraphs. We select the largest connected component (LCC) among all the connected components to perform the routing algorithms. The source and destination nodes are then randomly picked from the LCC. The statistics are obtained from the average of 10,000 runs. The same simulation setting is conducted for 5 different maximum transmission radii, which are 15, 20, 25, 30, and 35.

4.2 Observed Results

GG and RNG are the spanning subgraphs computed from UDG so that they both contain all the nodes of UDG. Thus, UDG, GG, and RNG also have the same number of nodes in their LCCs. Figure 3 shows the average number of nodes in the LCC for different radii. If the radius is set to 30, the average number of nodes in the LCC is very close to the total number of nodes, 75, in the entire graph. Figure 4 shows the average number

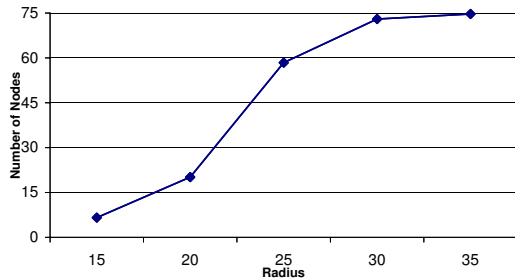


Figure 3: Average number of nodes in the LCC.

of edges in the LCC of each graph for different radii. As expected, the average number of edges increases as the radius increases. In Figures 5 and 6, we study the

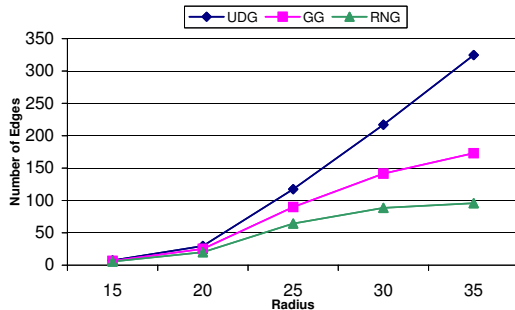


Figure 4: Average number of edges in the LCC of different graphs.

distribution of nodes in terms of the node degree. For

the radius of 25, Figure 5 shows the average percentages of nodes with various degrees of the nodes in the LCC of each graph (only the nodes in the LCC are considered). Figure 6 shows the average percentages of nodes with various degrees of the nodes in the LCC of UDG for different radii.

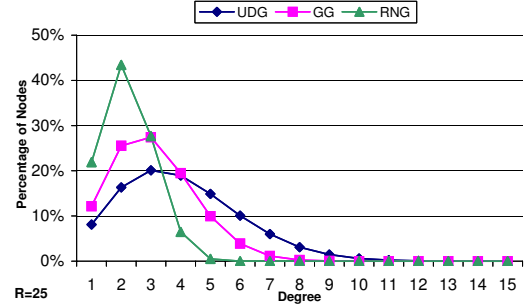


Figure 5: Distribution of nodes with various degrees in the LCC of different graphs for the radius of 25.

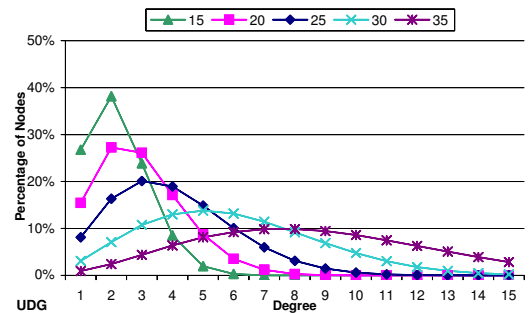


Figure 6: Distribution of nodes with various degrees in the LCC of UDG for different radii.

We compare the performance of the routing algorithms for different radii in Figure 7 and Figure 8. Figure 7 shows the delivery rate, given that the underlying network topology is UDG. For the radius of 25, the projective face routing algorithm performs significantly better than the other routing algorithms. Since the projected graphs on which the projective face routing algorithm performs are not necessarily planar graphs, we use a threshold value to terminate the routing process if the number of hops traversed exceeds 150. Interestingly, we also found that the curve of each routing algorithm for different radii is U-shaped (a parabola that opens upward). When the radius is small, the number of nodes in the LCC is small. The delivery rate decreases as the number of nodes in the LCC becomes larger. When the radius is 25, the number of nodes in the LCC almost reaches 80% of that of the entire graph. When we continue to increase the radius, the number of nodes in the LCC is nearly the same as the total number of nodes in the entire graph. However, the number of edges still increases (the average node degree increases) and this results in the increase of the delivery rate. Figure 8 shows the hop stretch factor. The hop stretch factor is close to 1 for the compass, greedy, ellipsoid, and most

forward routing algorithms even if the radius is set to different values. Therefore, the routing path traversed using these four algorithms is almost the same as the shortest path. In Figure 9 and Figure 10, the radius

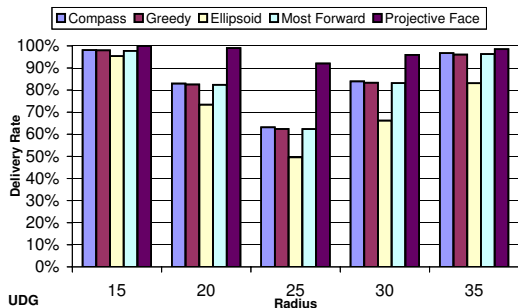


Figure 7: Delivery rate on UDG.

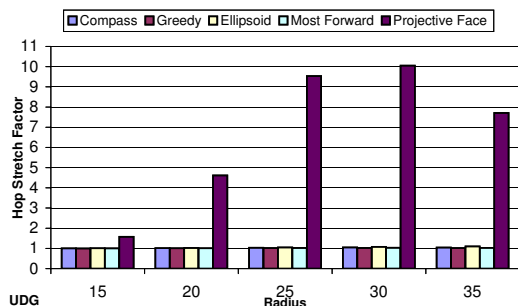


Figure 8: Hop stretch factor on UDG.

is set to 25. We compare the performance of the five routing algorithms on the three graphs.

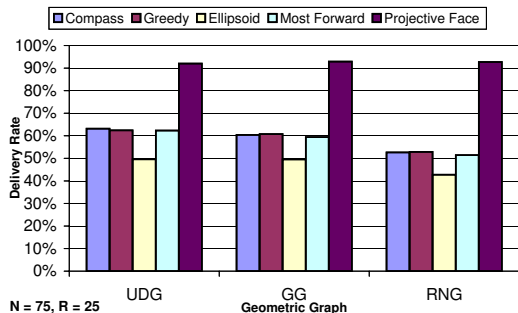


Figure 9: Delivery rate for the radius of 25 on different graphs.

5 Conclusion

We have studied the UDG and its associated spanning subgraphs in 3-D and extended the position-based routing algorithms to adapt to the context of 3-D. Our simulation showed that the ellipsoid routing algorithm does not give better delivery rate than the greedy routing algorithm as the number of nodes increases. This conclusion differs from what is claimed in [11]. Our proposed projective face routing algorithm performs significantly better in terms of delivery rate than the other routing

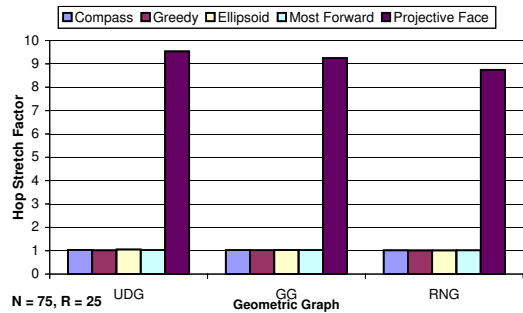


Figure 10: Hop stretch factor for the radius of 25 on different graphs.

algorithms. However, the projected graphs may have crossing edges that cannot be eliminated using only the local information. The delivery is thus not guaranteed. This open problem remains as future work.

References

- [1] L. Barrière, P. Fraigniaud, L. Narayanan, and J. Opatrny. Robust position-based routing in wireless ad hoc networks with irregular transmission ranges. *Wireless Communications and Mobile Computing Journal*, 3(2):141–153, 2003.
- [2] P. Bose, L. Devroye, W. S. Evans, and D. G. Kirkpatrick. On the spanning ratio of gabriel graphs and beta-skeletons. In *Proceedings of the 5th Latin American Symposium on Theoretical Informatics*, pages 479–493. Springer-Verlag, 2002.
- [3] P. Bose, P. Morin, I. Stojmenovic, and J. Urrutia. Routing with guaranteed delivery in ad hoc wireless networks. *Wireless Networks*, 7(6):609–616, 2001.
- [4] G. Finn. Routing and addressing problems in large metropolitan-scale internetworks. Technical report, ISI Research Report ISU/RR-87-180, March 1987.
- [5] K. Gabriel and R. Sokal. A new statistical approach to geographic variation analysis. *Systematic Zoology*, 18:259–278, 1969.
- [6] S. Giordano, I. Stojmenovic, and L. Blazevic. Position based routing algorithms for ad hoc networks: A taxonomy. In *Ad Hoc Wireless Networking*. Norwell, MA: Kluwer, 2003.
- [7] J. Jaromczyk and G. Toussaint. Relative neighborhood graphs and their relatives. In *Proceedings of the IEEE*, volume 80, pages 1502–1517, 1992.
- [8] B. Karp and H. Kung. GPSR: Greedy perimeter stateless routing for wireless networks. In *Proceedings of the 6th annual international conference on Mobile computing and networking*, pages 243–254. ACM Press, 2000.
- [9] E. Kranakis, H. Singh, and J. Urrutia. Compass routing on geometric networks. In *Proceedings of the 11th Canadian Conference on Computational Geometry*, pages 51–54, Vancouver, August 1999.
- [10] H. Takagi and L. Kleinrock. Optimal transmission ranges for randomly distributed packet radio terminals. *IEEE Transactions on Communications*, COM-32(3):246–257, March 1984.
- [11] K. Yamazaki and K. Sezaki. The proposal of geographical routing protocols for location-aware services. *Electronics and Communications in Japan*, 87(4), 2004.